LEVELS IN ^{239}Np AND ^{239}Pu STUDIED BY COINCIDENCE SPECTROMETRY OF GAMMA TRANSITIONS FOLLOWING ^{243}Am DECAY

A THESIS

Presented to

The Faculty of the Division of Graduate

Studies and Research

by

Jerry Clark Pate

In Partial Fulfillment

of the Requirements for the Degree

Master of Science in Chemistry

Georgia Institute of Technology

June, 1974

LEVELS IN ^{239}Np AND ^{239}Pu STUDIED BY COINCIDENCE SPECTROMETRY OF GAMMA TRANSITIONS FOLLOWING ^{243}Am DECAY

Approved:

R. W. Fink, Chairman

D. A. McClure

H. M. Neumann

Date approved by Chairman: MAY 10 1974

ACKNOWLEDGMENTS

I would like to recognize those individuals and organizations whose support made this research possible.

I wish to express my sincere appreciation to my thesis advisor, Professor R. W. Fink, for his continuing interest and encouragement.

My special thanks are due to Professor D. A. McClure who provided the computer based detector system and many of the computer programs used in the data analysis and without whose patience, guidance, and never-ending assistance, this work could not have been completed.

Professor H. M. Neumann provided invaluable advice on radiochemical procedures and offered many suggestions in his review of the manuscript.

A great deal of credit is due to Dr. K. R. Baker who served not only as a knowledgeable technical advisor in a postdoctoral capabity, but as a trusted friend and co-worker.

Dr. R. M. Harbour of the Savannah River Laboratory provided the solution from which the americium source was prepared.

Frequent interactions with Drs. J. Wood and A. Xenoulis nurtured a better understanding of theoretical nuclear chemistry.

The friendship of Messrs. F. Tolea, B. Chew, D. Nix, G. Gowdy, and others will always be remembered.

I am thankful to Mrs. Lydia Geeslin for the typing of the manuscript.

This research project was supported by AEC Contract No. AT(40-1)-3346.

I wish to thank the Department of the Army for making my graduate training possible.

I am forever indebted to my loving wife, Barbara, for her constant support and encouragement throughout this entire project.

TABLE OF CONTENTS

LIST OF TABLES

LIST OF ILLUSTRATIONS

SUMMARY

The nuclide ^{243}Am undergoes alpha decay with a half-life of 7.950×10^3 years to 2.346 day ^{239}Np which beta decays to 2.44×10^4 year ^{239}Pu. The present investigation represents a study of the excited states in ^{239}Np and ^{239}Pu populated by ^{243}Am decay.

General features of the published level schemes for these nuclei are consistent with predictions of the Nilsson and collective models; however, there remain many undiscovered transitions and ambiguous or uncertain level assignments. In order to confirm current theoretical models which account for nuclear level assignments in these nuclei, these gamma transitions and their levels are established with certainty.

In the present work, the decay of ^{243}Am is investigated by (i) radiochemical purification, (ii) high resolution gamma singles spectrometry, and (iii) two-parameter gamma-gamma coincidence spectrometry. The present equipment, composed of two Ge(Li) semiconductor detectors, a 4096-channel, two-parameter analyzer, and a PDP-8/e computer system, permitted considerable improvement in accuracy and sensitivity over previous work on these nuclei.

CHAPTER I

INTRODUCTION

The element americium was discovered during experiments conducted in late 1944 at the Metallurgical Laboratory (now Argonne National Laboratory) of the University of Chicago by G. T. Seaborg, R. A. James, L. O. Morgan, and A. Ghiorso.[1,2] It was chemically separated from products of the neutron irradiation of plutonium, an element whose properties had received extensive investigation because of the military implications of the slow neutron fission reaction. As element number 95, it was named americium (Am) after the Americas on the basis of its position as the sixth member of the actinide rare earth series, analogous to europium of the lanthanide rare earths.[2] The isotope ^{243}Am is particularly suited for chemical study because of its relatively long (7.95×10^3 y) half-life. The nuclear properties of ^{239}Np and ^{239}Pu, from decay of ^{243}Am, have been chosen as the subject of this investigation. Early work on the nuclear decay schemes of ^{239}Np and ^{239}Pu is summarized in Ref. (3) and (4).

Both ^{243}Am and its daughter products lie in the heavy element region ($A > 225$), where nuclei have been found to have pronounced spheroidal deformations and properties which have yielded significant contributions to the development of various theoretical nuclear models. These models attempt to characterize, under a set of rather simple assumptions, the complex forces acting in these nuclei. Refinement of the theoretical predictions of these nuclear models has been achieved by careful and

detailed accumulation of extensive experimental data, such as obtained in this and similar studies.

The motion of single nucleons in spherical nuclei close to closed shells has been described by various refinements of the fundamental, independent particle model. An important interaction first proposed independently by Mayer[5] and by Haxel, Jensen, and Suess[6] in 1948, assumed strong spin-orbit coupling forces for individual nucleons. Theory was then able to predict the phenomenologically observed stability of independent particle states corresponding to the "magic number" nuclei.

A major component of the nucleon-nucleon residual interaction manifests itself as an energy gap observed between the ground state and the first excited state in even-even nuclei. This energy gap is the result of a strong, short-range, attractive force between nucleons of the same shell model state and is referred to as the pairing interaction.

Empirical evidence seems to indicate that long range effects of the nuclear potential lead to a correlated motion of the nucleons in an average potential force field. This results in nuclear excitation levels which have energy below that expected for single particle excitations. These levels are classified in terms of rotations or vibrations of the nucleus as a whole.

As more accurate measurements of the quadrupole moments of certain nuclei became available, their large magnitude indicated that many nuclei are not spherically symmetric in shape, but are assymetrically deformed. The average potential experienced by individual nucleons in these nuclei is assumed to approximate closely the deformed nuclear shape. Nilsson[7] first described nuclei in terms of the motion of unpaired nucleons outside

of a distorted central nuclear core.

Further refinements of the nuclear models have included various perturbation effects chosen on the basis of physical intuition and parameterized to fit the experimentally observed nuclear properties of various nuclei. As state-of-the-art electronic equipment and radiation detectors have advanced rapidly in the past few years, so have the quantity and precision of experimentally measured and determined nuclear properties. These new data provide very sensitive and critical tests for any final, comprehensive, working, nuclear model.

There is little recent published data concerning the low energy level structure of ^{239}Np, the alpha decay product of ^{243}Am. Engelkemier has conducted the most recent studies of the decay of this nuclide by α-γ coincidence techniques[8] and by conversion electron spectroscopy.[9] He proposed several new transitions and indicated possible new energy levels. The present investigation attempts to extend this and earlier research on this decay scheme by accurately measuring the low energy gamma-ray spectrum with both small volume (high resolution) and large volume (high efficiency) Ge(Li) detectors. This study of the gamma-ray singles and gamma-gamma coincidence spectra associated with the alpha decay of ^{243}Am to levels in ^{239}Np and subsequent beta decay to levels in ^{239}Pu (see Fig. 1), attempts to elucidate further the level schemes of these product nuclei.

Chapter II briefly outlines the theory of the low energy structure of deformed (heavy) odd-mass nuclei and principles of gamma-ray spectroscopy.

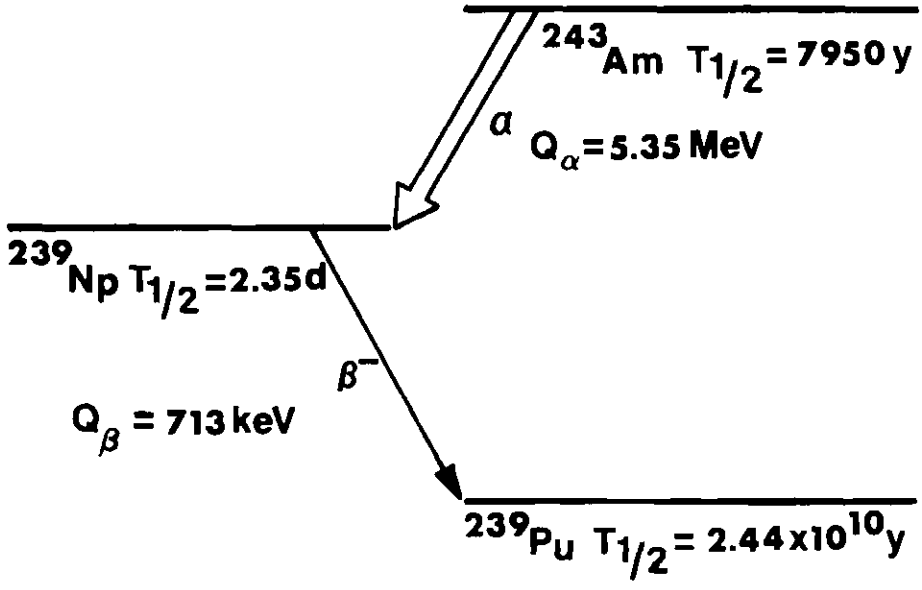

Figure 1. ^{243}Am Decay Scheme Showing Ground State Paths Only

Chapter III presents the experimental procedures and methods of data reduction adopted in the present investigation, describing the equipment utilized, the method of source preparation, and the singles and gamma-gamma coincidence measurements.

Chapter IV is a discussion of the results of this investigation and their interpretation in the light of currently accepted level schemes and models of nuclear behavior in this region.

CHAPTER II

THEORETICAL BACKGROUND

The nucleus of an atom is a many body structure of extraordinary complexity. The principal forces operating within the nucleus are the strong (nuclear binding) forces, the electrostatic (Coulomb) force, and the weak interaction force. Because the properties of nuclear forces are not well known, various simplifying assumptions concerning coordinated interactions of nucleons within the nucleus have been made. Each set of assumptions has resulted in a different nuclear model which can be successfully applied to only a restricted number of nuclei.

The nucleus ^{243}Am, with 95 protons and 148 neutrons, lies in a region of nuclei where large electric quadrupole moments have been measured, indicating a large degree of nuclear deformation. Nuclei in this region are best described by the Nilsson model for single-particle shell states in deformed nuclei, and by the Bohr-Mottelson collective model for rotational and vibrational motion.

In order to describe the single-particle motion of a nucleon inside a nucleus, it is first necessary to find a suitable expression for the potential energy of the nucleon. As a first approximation, each nucleon is described as moving in a potential field which is an average of the interactions of that nucleon with all of the other (A-1) nucleons within the nucleus.

This potential is usually considered to be spherically symmetric,

with the form either of a three-dimensional isotropic harmonic oscillator or of a square well. The true nuclear potential is thought to lie somewhere between these two limits.

For the harmonic oscillator potential, the energy eigenvalues are given by the expression:

$$E_N = (N + 3/2)\hbar\omega \tag{1}$$

$\hbar\omega$ is a quantum of vibrational motion, with

$$\omega = 2\pi f \tag{2}$$

where f is the frequency of vibration and N, the principal quantum number, is given by:

$$N = \ell + 2(n-1) \tag{3}$$

The number n is equal to the number of nodes in the radial wave function and ℓ is the orbital angular momentum quantum number. For each energy, E_N, there exists a degenerate set of single particle levels; the levels having different values of n and ℓ. There is further degeneracy in the magnetic quantum number, m_s. The total degeneracy of each energy state is given by the expression (2j+1), where j is the total angular momentum. Since nucleons have spin, s, where

$$s = 1/2 \tag{4}$$

and

$$j = \ell \pm s = \ell \pm 1/2, \tag{5}$$

the total number of nucleons of each kind with the same n and ℓ values is $2(2\ell+1)$. This gives the correct level ordering for only the lighter nuclei.

A major advancement was recognition, by Mayer[5] and by Haxel, Jensen, and Suess,[6] of the importance of strong spin-orbit coupling $(-K\vec{\ell}\cdot\vec{s})$, where

$$j_{max} = \ell + s \tag{6}$$

$$j_{min} = \ell - s \tag{7}$$

i.e., states with $\ell + 1/2$ are more tightly bound than states with $\ell - 1/2$.

The nuclear potential was written as,

$$V = 1/2\ m\omega_o^2 r^2 + \hbar\omega_o\ [C\vec{\ell}\cdot\vec{s} + D\vec{\ell}\cdot\vec{\ell}] \tag{8}$$

where C and D are negative constants, the values of which are adjusted to fit the empirical data for each shell in both the neutron and proton filling order, and

$$\omega_o = \frac{k}{m} \tag{9}$$

where m is the mass of the nucleon and k is a force constant which describes the average single-particle field. The effect of strong spin-orbit coupling is to give different occupation numbers for closed shells. The order of the energy levels within a shell depends sensitively on the form of the potential well and on the magnitude of the spin-orbit coupling assumed.

Nilsson[7] chose a non-spherical, modified harmonic oscillator potential that produced agreement with empirical data over a greater range of mass numbers. His choice for the Hamiltonian (in Cartesian coordinates) of a prolate or oblate spheroidal nucleus is given as:

$$H_{sph} = \frac{p^2}{2m} + 1/2\ [k_\perp\ (x^2+y^2) + k_z z^2] + C\vec{\ell}\cdot\vec{s} + D\vec{\ell}^2 \qquad (10)$$

where the force constant, $k_\perp = k_x = k_y$. In this expression, $\frac{p^2}{2m}$ is the kinetic energy of the nucleon, $1/2\ [k_\perp\ (x^2+y^2) + k_z z^2]$ is the deformed nuclear potential, $C\vec{\ell}\cdot\vec{s}$ is the spin-orbit coupling term, and the $D\vec{\ell}^2$ term distorts (i.e., flattens) the nuclear potential. The inclusion of the $D\vec{\ell}^2$ term had the effect of lowering the nuclear potential just inside the nuclear edge.

Spheroidal deformation of the even-even core of the nucleus means that the odd nucleon no longer moves in a spherically symmetric potential and, therefore, its orbital angular momentum (ℓ) and total angular momentum (j) are no longer conserved. However, the total angular momentum of the system must be conserved, which leads to the conclusion that the spheroidal core must have angular momentum coupled to that of the odd nucleon. Parity (π) is still a good quantum number, where the parity is determined as:

$$\pi = (-1)^N \qquad (11)$$

The parity is designated (+) or (-) depending on the even or odd character of the principal quantum number.

The Nilsson quantum numbers, as shown in Fig. 2, are:

Ω which is the projection of $\vec{j}$, the angular momentum of the odd nucleon, on the nuclear symmetry axis;

Λ which is the projection of $\vec{\ell}$, the orbital angular momentum of the odd nucleon, on the nuclear symmetry axis, where $\Lambda = \Omega \pm 1/2$;

Σ which is the projection of $\vec{s}$, the intrinsic nuclear spin, on the nuclear symmetry axis;

N the principal quantum number, which is equal to the total number of nodes in the wave function;

n_z the number of nodal planes perpendicular to the symmetry axis, from the energy eigenvalues of the Nilsson Hamiltonian as given by:

$$E_N = (n_\perp + 1)\hbar\omega_\perp + (n_z + 1/2)\hbar\omega_z \tag{12}$$

where $\omega_\perp$ and ω_z are harmonic oscillator constants and

$$N = n_\perp + n_z \tag{13}$$

The energy levels of a nucleus are identified by the values of Ω and parity (π) and by the quantum numbers N, n_z, and Λ. They are often labeled as $\Omega^\pi[N,n_z,\Lambda]$.

The eigenvalues corresponding to these eigenstates of the Nilsson Hamiltonian are usually displayed as a plot of energy in units of $\hbar\omega_o$ versus nuclear deformation (ε). This parameterization ($\hbar\omega_o$) serves as an energy scale factor and is dictated by the single-particle level density of nuclei. The Nilsson diagram pertinent to the mass region $A \simeq 243$ is given in Fig. 3. This diagram is taken from Ref. (10). The energy

levels are labeled by $[N,n_z,\Lambda,\Omega]$.

The ground state of ^{239}Np is $5/2^+[642]$ and that of ^{243}Am is $5/2^-[523]$. The proton states in these nuclei lie at a nuclear deformation of $\epsilon \approx 0.25$ in Fig. 3, corresponding to proton numbers 93 and 95.[11] The Nilsson quantum numbers, [523], define the ground state as follows: $N = 5$, $n_z = 2$, and since $N - n_z = 3$ (odd), Λ must be 3, i.e., $\Omega + 1/2$. The nuclide ^{239}Pu has a ground state of $1/2^+[631]$ that is similarly defined by its odd neutron state.

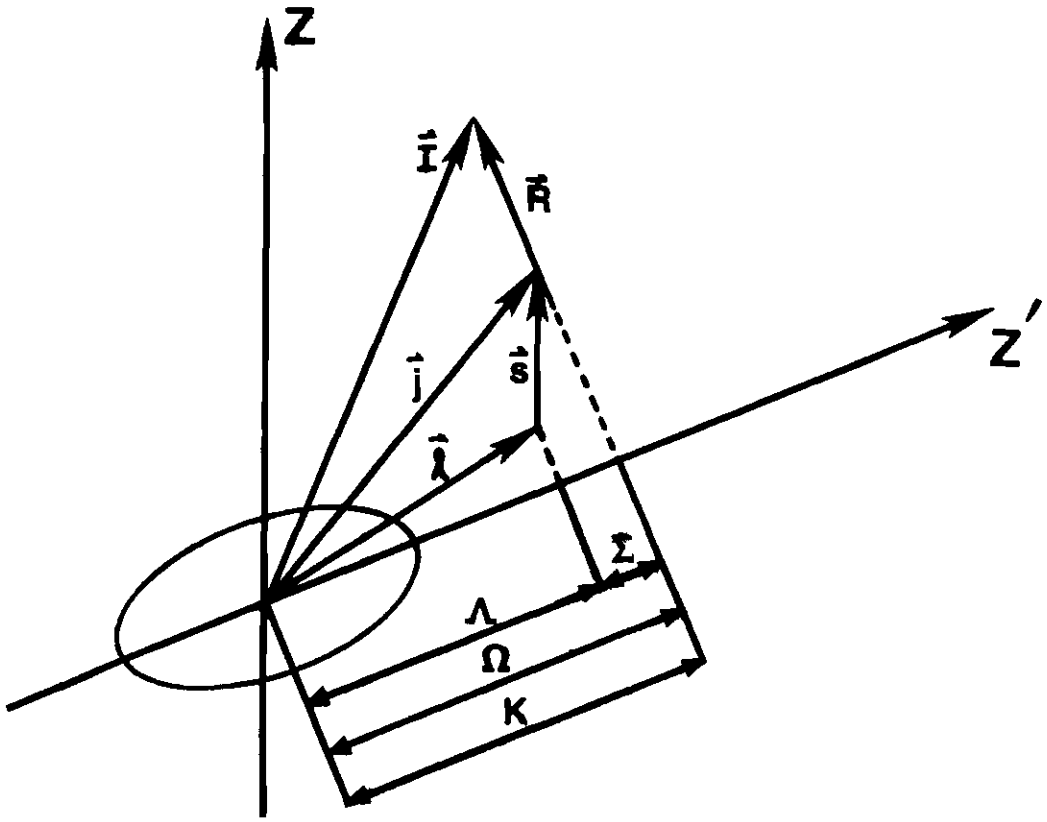

Figure 2. Angular Momentum Coupling in the Nucleus and Quantum Numbers for Deformed Nuclei

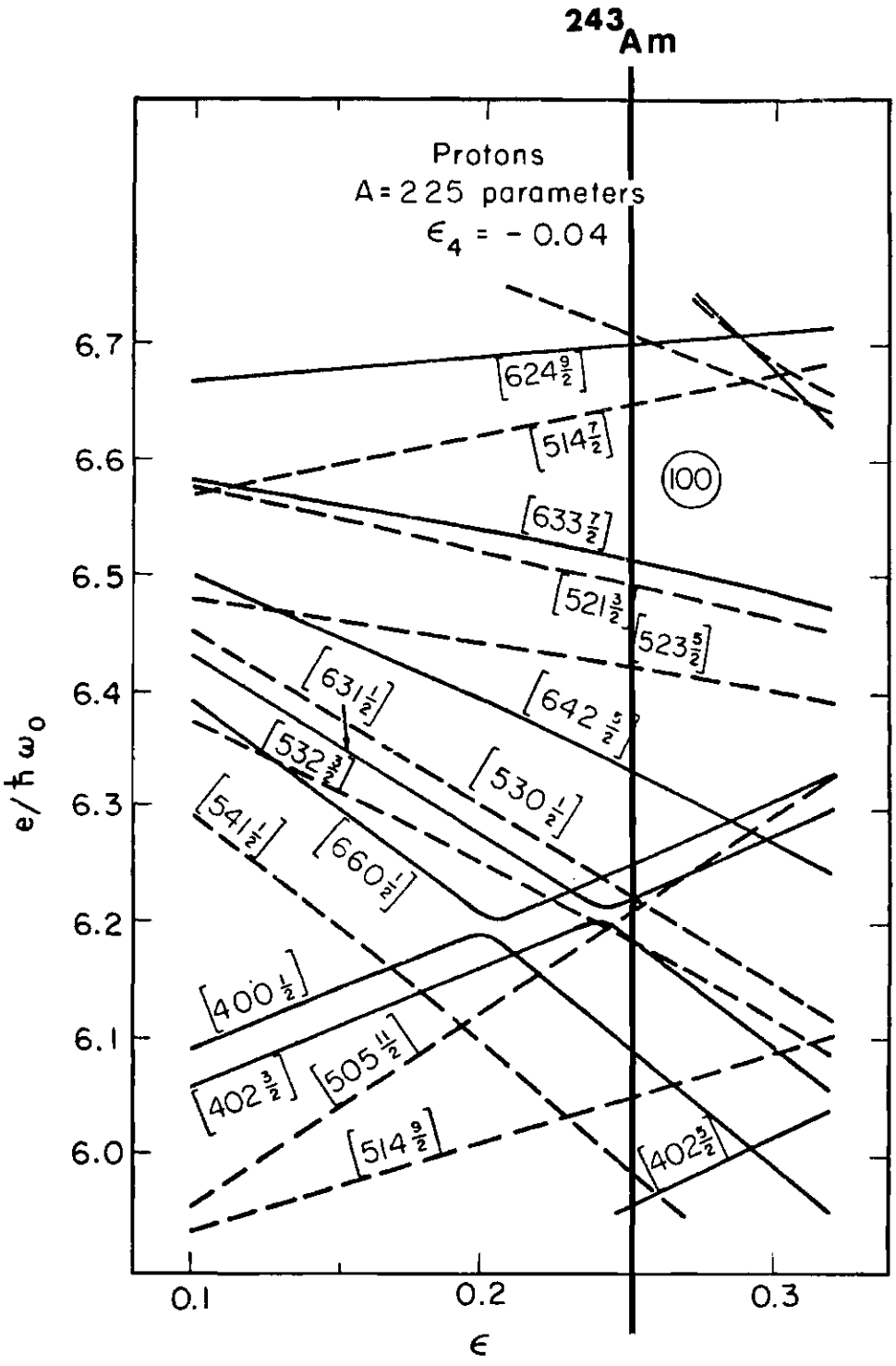

Figure 3. Nilsson Diagram for Mass Region A ≅ 243 Indicating the Position of ^{243}Am with Nuclear Deformation, ε ≅ 0.25

CHAPTER III

EXPERIMENTAL METHODS AND DATA REDUCTION

The collection and analysis of data on ^{243}Am decay proceeded in four distinct phases. The radioactive source was first prepared. The detector and electronic instrumentation were then calibrated by plotting an efficiency curve using known standard sources. Singles spectra were taken to determine the energies and intensities of individual gamma transitions. Coincidence data were then used to place the transitions in the decay schemes.

1.1 Source Preparation

Chemical separation of ^{243}Am from its nuclear decay products was performed on a five (5) milliliter solution of ^{243}Am in 1M HNO_3 provided by Dr. R. M. Harbour, Analytical Chemistry Division, Savannah River Plant. This solution contained ^{243}Am in equilibrium with its daughter products and had 1.573×10^7 dis/min•ml gross alpha activity and 1.363×10^7 dis/min•ml ^{243}Am activity.

Lanthanum hydroxide [$La(OH)_3$] was used as a carrier, to isolate the actinides from the gross activity. The $La(OH)_3$ was then dissolved in HNO_3 and lanthanum was reprecipitated with ammonium fluoride [NH_4F]. The lanthanum fluoride precipitate, containing $^{243}Am(VI)$, $^{239}Np(IV)$, and $^{239}Pu(IV)$ was dissolved in aluminum nitrate [$Al(NO_3)_3$] and diluted with 1M HNO_3. From this solution, ^{239}Np and ^{239}Pu were extracted with 0.5M

thenoyltrifluoroacetone (TTA) in xylene. A comprehensive investigation of TTA extraction coefficients for 48 elements has been given in the literature, see Ref. (12).

The experimental procedure consisted of three parts: (1) the acid concentration of HNO_3 was adjusted to 1M and $^{239}Pu(VI)$ and $^{239}Np(V)$ were reduced with ferrous sulfamate $[Fe(NH_2SO_3)_2]$ to $^{239}Pu(IV)$ and $^{239}Np(IV)$, respectively; (2) $^{239}Np(IV)$ and $^{239}Pu(IV)$ were quantitatively isolated by solvent extraction with 0.5M TTA in xylene; and (3) the aqueous extract, containing ^{243}Am was analyzed by gamma-ray spectroscopy, using a small volume Ge(Li) detector (see Sect. 1.3).

Complete separation of $^{243}Am(V)$ from its daughters was assured by close control of the acid concentration to 1 ± 0.1M and by repeating the extraction step as required. The extraction procedure[13] follows.

(1) An aliquot of the radioactive ^{243}Am solution having 10^3 to 10^4 dis/min of alpha count rate was pipetted into a 15 ml centrifuge cone.

(2) Distilled water or HNO_3 was added so that at the end of the next step the acid concentration was 1M.

(3) One ml of 2M ferrous sulfamate $[Fe(NH_2SO_3)_2]$ solution was added as a reducing agent. The solution was thoroughly mixed and allowed to stand for five minutes.

(4) Three ml of 0.5M TTA in xylene was added and stirred vigorously for five minutes.

(5) The aqueous and organic phases were allowed to separate and the organic phase, containing $^{239}Pu(IV)$ and $^{239}Np(IV)$, was removed with a transfer pipette.

(6) Steps (2) through (5) were repeated three to four times to achieve a complete separation of the ^{243}Am activity.

Upon concentration by evaporation, an aliquot of the aqueous phase, containing an amount of ^{243}Am equivalent to 10^3 dis/min was added dropwise to a Mylar film supported on a plastic ring and heated to dryness. The source was then allowed to cool and the radioactive deposit was sprayed with a thin film of acrylic resin prior to counting.

Alternatively, because of the short half-life (2.35 d) of the ^{239}Np daughter, the freshly separated aqueous phase was immediately counted in the liquid state.

By comparison with an electroplated ^{243}Am source,* in equilibrium with its daughters, the fresh chemically separated source exhibited a large reduction (< 10 dis/min ^{239}Np per 10^6 dis/min ^{243}Am at the instant of separation) in the intensity of Pu K x rays** arising from 2.35 d ^{239}Np decay, relative to the 43.531 and 74.673 keV gamma rays in ^{243}Am decay. Details of the singles spectroscopy are discussed in Sect. 1.3 below. These results show that an excellent separation of the 2.35 d ^{239}Np and long-lived ^{239}Pu daughters was achieved by this radiochemical procedure.

A further evidence that the new gamma rays reported in Sect. 1.3 arise from ^{243}Am decay, and not from some extraneous impurity such as a fission product, is obtained from the observation that the growth of these gamma rays requires approximately eight days to achieve radioactive equilibrium, in agreement with the predicted t_{max} for growth of a 2.35 day

*Purchased several years earlier from the Oak Ridge National Laboratory, Oak Ridge, Tennessee.

**Pu $K\alpha_1$, $K\alpha_2$, $K\beta_1'$, and $K\beta_2'$ x rays at 103.65, 99.46, 117.15, and 120.59 keV, respectively.

daughter from the 7950 year ^{243}Am parent.

1.2 Detector Efficiency Calibration

Since construction of a decay scheme requires both accurate determination of photopeak gamma-ray intensities and energies, it was necessary to determine the relative efficiency of the two detectors used in this work. This was done for the ORTEC Ge(HP) detector* and for the ORTEC large volume, true coaxial Ge(Li) detector.**

The detector photopeak response curves (see Fig. 4) were established with a set of standard gamma-ray sources of known activity consisting of ^{241}Am, ^{57}Co, ^{60}Co, ^{137}Cs, ^{54}Mn, ^{22}Na, and ^{88}Y provided by the International Atomic Energy Agency (IAEA), Vienna, and a ^{182}Ta source produced by the ^{181}Ta (n,γ) ^{182}Ta reaction in the Georgia Tech Research Reactor (see Table 1). Also, many of the gamma rays in ^{243}Am decay have precisely determined intensities that can be used as internal relative efficiency standards.[14)]

The standard sources were placed individually at a fixed distance (2.5 cm) from the detectors and counted for a known time. Since the activity and decay characteristics of these standard sources are accurately known to 1-2 percent, the efficiency of the detectors can be calculated from the following relationship:

$$\epsilon_{(E)} = C_E/(N_E\ N_o)$$

*A 6 mm active diameter x 3.5 mm sensitive depth, high resolution intrinsic germanium detector with a resolution of 0.50 keV FWHM at 59.54 keV.

**A 46.5 mm active diameter x 48.5 mm active depth, true coaxial Ge(Li) detector, with a resolution of 2.1 keV FWHM at 1.33 MeV and an efficiency of 14.7 percent for the 661 keV line in ^{137}Cs decay, compared to a 7.5 cm x 7.5 cm NaI(Tl) detector.

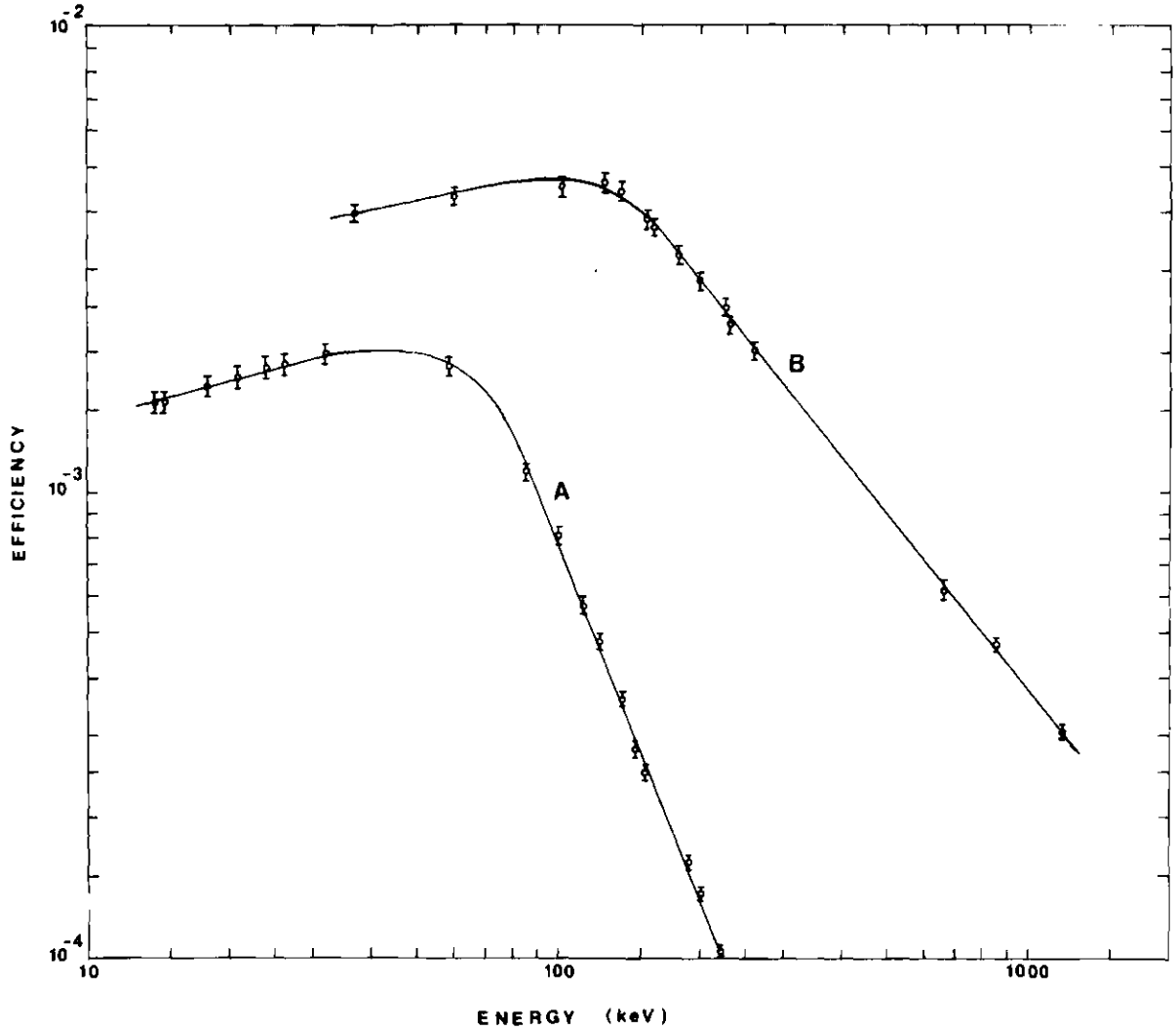

Figure 4. Detector Efficiency Curves (Curve A represents the relative detection efficiency of the intrinsic Ge(HP) low energy photon detector [6 mm active dia x 3.5 mm sensitive depth; resolution 0.50 keV FWHM at 59.54 keV] at the distance used in the present work (2.5 cm). Curve B represents the absolute detection efficiency of the large volume, coaxial Ge(Li) gamma-ray detector [46.5 mm active dia x 48.5 mm sensitive depth; 14.7% efficient for the ^{137}Cs 661 keV line relative to 7.5 x 7.5 cm NaI(Tl); resolution 2.1 keV FWHM at 1.33 MeV] at the distance used in the present work (2.5 cm).)

Table 1. Standard Sources Used in the Detector Efficiency Calibration

Nuclide	Photon Energy (keV)	Photons Emitted per Decay*
^{241}Am	13.9	0.135 ± 0.003
	17.8	0.202 ± 0.004
	20.8	0.050 ± 0.001
	26.4	0.025 ± 0.002
	59.54	0.359 ± 0.006
^{57}Co	14.36	0.095 ± 0.002
	121.97	0.856 ± 0.003
	136.33	0.1075 ± 0.003
^{60}Co	1173.23	0.9974 ± 0.0005
	1332.49	0.9985 ± 0.0003
^{137}Cs	32.1	0.0567 ± 0.002
	32.9	0.0702 ± 0.0022
	36.5	0.01345 ± 0.00048
	661.635	0.851 ± 0.005
^{54}Mn	834.81	1.000
^{22}Na	1274.55	0.9995 ± 0.0002
^{182}Ta	84.68	18.5
	100.1	100.0
	113.7	13.9
	116.4	3.17
	152.4	51.5
	156.4	19.8
	179.4	23.3
	198.35	10.8
	222.1	55.7
	229.3	28.1
	264.1	26.4
^{88}Y	14.4	0.6340 ± 0.0032
	898.04	0.914 ± 0.007

*All values are taken from Ref. 15.

where C_E is the number of counts detected in the photopeak of energy E, N_E is the number of photons of energy E emitted per disintegration, and N_o is the disintegration rate per second.

The detector photopeak response curves give the relative full energy peak detection efficiencies of the Ge(Li) detectors as a function of photon energy. These curves show the typical efficiency response of semiconductor detectors. The drop-off at low energy is due to absorption of the gamma rays in air, the beryllium window, the gold contact layer, and in the insensitive (dead) germanium layer. The drop-off at high energy is due to the decreased photoelectric cross section at high energy.

1.3 Gamma-Ray Singles Measurements

As gamma rays, emitted by a decaying nuclide, enter the germanium semiconductor detector, they interact by one (or more) of three processes: photoelectric effect, Compton scattering, or pair production.

In the photoelectric process, the gamma ray gives up its energy to an inner shell electron. The kinetic energy of this primary electron is then transferred to secondary electrons, resulting in their elevation to the conduction band. The bias voltage carries this current away to the preamplifier, producing a signal proportional to the energy deposited in the sensitive volume of the detector crystal.

In Compton scattering, the gamma ray is scattered by an outer shell electron. If the scattered photon escapes from the detector without further interaction, the energy deposited by the gamma ray is equal to the kinetic energy of the primary electron, which will have a maximum value when the photon is scattered through 180 degrees. Therefore, this

Compton edge in a gamma-ray spectrum represents the maximum transfer of energy to the electron in a single encounter. Multiple scattering of secondary photons may take place in a large crystal in a short time interval. If all of the energy of the primary gamma ray is transferred to the crystal in this way, the signal is essentially the same as if it had been photoelectrically absorbed.

Pair production can occur if the energy of the gamma ray is greater than 1.022 MeV. In the present case, however, no gamma rays of energy sufficient to produce pairs are present.

Voltage signals, generated by the above processes, are transmitted from a preamplifier to be shaped and amplified by a linear amplifier. The height of the signal is normally a very precise measure of the energy deposited in the sensitive volume of the detector. The gamma-ray spectrum is obtained by digitizing these pulses in an analog-to-digital converter (ADC) within a multichannel analyzer (MCA) and storing the counts in its 2048-channel memory (see Fig. 5)

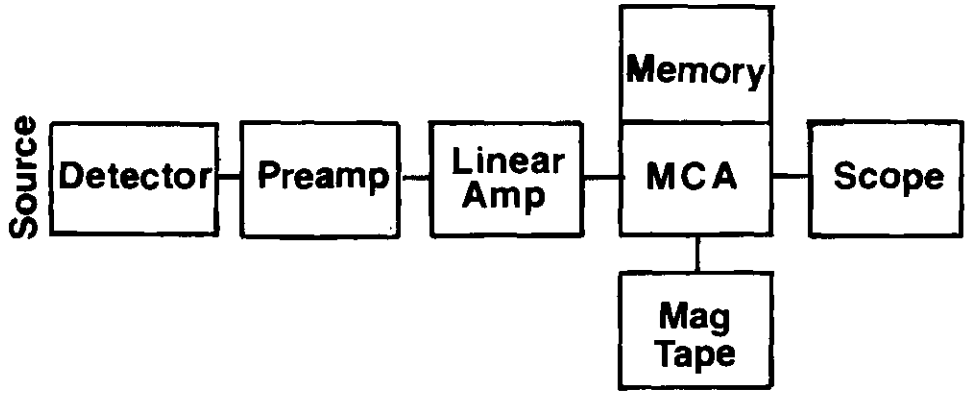

Figure 5. Block Diagram of Gamma-Ray Singles System

The spectrum can then be recorded on magnetic tape and converted to computer cards for analysis. The term "singles spectra" refers to gamma-ray spectra taken with a single detector, having no coincidence requirement imposed on the gamma transitions.

Gamma-ray photopeaks in the singles spectra ride on a Compton continuum which is greater at lower energies because of summing of the higher energy gamma contribution to the continuum and because of the more frequent occurrence of small angle scattering.

In the present work, singles measurements were made with both a large volume and a small volume germanium detector. The high efficiency of the large volume detector permitted good counting statistics for the high energy gamma rays, within a reasonable acquisition time. However, the very high resolution of the small volume detector permitted the observation of multiplets which had not previously been resolved. The larger peak-to-continuum ratio of the small volume detector also made visible low energy photopeaks, which are hidden in the high Compton background spectra from the large volume detectors. Thus, the combination of both detectors revealed many new transitions which had not been reported previously.

Energies of the gamma rays observed in this work were determined using a computer program employing a Gaussian peak shape to fit the peak centroids to known energy transitions in the decay scheme. The levels of ^{239}Np populated by the beta decay of ^{239}U had been studied previously with a bent crystal gamma spectrometer.[16] The precise values of gamma-ray energies so obtained, 74.673 and 43.531 (and by difference, 31.142)

keV, were used as internal standards.

Accurate determination of energies of individual gamma transitions enables these transitions to be placed more unambiguously in the decay scheme. The gamma-ray energies and relative intensities determined in this investigation and, for comparision, comparable published values for this decay are presented in Table 2.

The gamma-ray energies in Table 2 represent average energy values of two separate singles measurements with the small volume (high resolution) Ge(HP) detector (see Sect. 1.2) over the energy range 20 to 334 keV using the electroplated ^{243}Am source. A singles gamma-ray spectrum taken with this detector using the same source is shown in Fig. 6.

Figure 6 displays the low energy gamma transitions observed in the present work. Prominent in this spectrum are the Pu x rays: L x rays (12 to 22 keV), $K\alpha_2$ (99.46 keV), $K\alpha_1$ (103.65 keV), $K\beta_1'$ (117.15 keV), and $K\beta_2'$ (120.59 keV). Gamma rays from ^{241}Am, a contaminant present in the electroplated ^{243}Am source, are identified in the spectrum at 26.40 and 59.54 keV. The gamma rays at 31.10, 43.53, 74.67, 86.79, 117.60, and 142.18 keV are established transitions in the ^{239}Np level scheme. The gamma rays at 44.55, 49.44, 57.32, 61.51, 67.04, 106.29, 181.83, 209.86, 226.64, and 228.11 are also well established transitions in the daughter, ^{239}Pu, level scheme. The 106.29 keV gamma ray is a doublet with most of its intensity depopulating the 391.52 keV level and the remaining intensity depopulating the 163.79 keV level (see Fig. 14, Chapter IV).

The 116.41 keV gamma ray was clearly resolved from the Pu $K\beta_1'$ x ray and the 117.60 keV ^{239}Np gamma ray using the small volume Ge(HP) detector. The 121.70 keV gamma ray was also resolved from the Pu $K\beta_2'$ x ray.

Table 2. Gamma-Ray Energies in ^{243}Am Decay

Present Work		I. Ahmad and M. Wahlgren[14] 1972		J. R. Van Hise and D. Engelkemeir[8] 1968	
Energy	Intensity[a]	Energy	Intensity[b]	Energy	Intensity[b]
31.10	0.11 ± 0.01			31.142	0.05
43.1 *				43.1	
43.53	8.40 ± 0.06	43.531	8.3 ± 0.5	43.531	8.7
44.55	0.18 ± 0.02				
46.73	0.088 ± 0.009				
49.44	0.17 ± 0.02				
				50.6	0.0044
				55.4	0.014
57.32	0.18 ± 0.02				
61.51	2.0 ± 0.2				
64.84	0.35 ± 0.04				
67.04	0.43 ± 0.04				
74.67	100.0	74.673	100.0 ± 4.5	74.673	100.0
77.95	0.35 ± 0.03				
80.24	0.084 ± 0.008				
86.79	0.51 ± 0.05			86.7	0.61
99.67	18.69 ± 1.8	99.536	21.97 ± 0.9	99.536	23.8
103.88	29.25 ± 2.9	103.750	33.64 ± 1.2		
106.29	38.59 ± 3.8	106.14	42.12 ± 1.4		

Table 2. (Continued)

Present Work		I. Ahmad and M. Wahlgren[14] 1972		J. R. Van Hise and D. Engelkemeir[8] 1968	
Energy	Intensity[a]	Energy	Intensity[b]	Energy	Intensity[b]
116.41	4.0 ± 0.4				
117.15	8.4 ± 0.5	117.1	13.48 ± 0.6		
117.60	0.84 ± 0.12			117.8	1.23
120.74	3.4 ± 0.3	120.6	4.19 ± 0.2		
121.70	1.0 ± 0.1				
142.18	0.19 ± 0.02			142.0	0.21
				169.0	0.0019
181.83	0.06 ± 0.02	181.71	0.11 ± 0.01		
				195.0	0.0014
209.86	4.68 ± 0.05	209.76	5.18 ± 0.2		
226.64	3.75 ± 0.70				
228.11	15.54 ± 1.2	228.20	17.27 ± 0.5		
254.46	0.15 ± 0.02	254.41	0.17 ± 0.02		
272.87	0.11 ± 0.05	272.87	0.12 ± 0.02		
277.66	20.9 ± 1.9	277.62	21.97 ± 0.6		
285.54	1.11 ± 0.14	285.47	1.15 ± 0.03		
316.05	2.32 ± 0.25	315.91	2.30 ± 0.08		
334.49[†]	3.09 ± 0.30	334.33	2.95 ± 0.1		

[a] Photon intensities relative to 100.0 for the 74.67 keV gamma ray. [b] Photon intensities originally reported in terms of photons emitted per 100 alpha decays have been recalculated relative to 100.0 for the 74.67 keV gamma ray. [*] Resolved in the coincidence spectra. [†] E_γ and I_γ in the energy range $334 < E_\gamma < 661.59$ keV were determined and found to confirm current published values (Ref. 4).

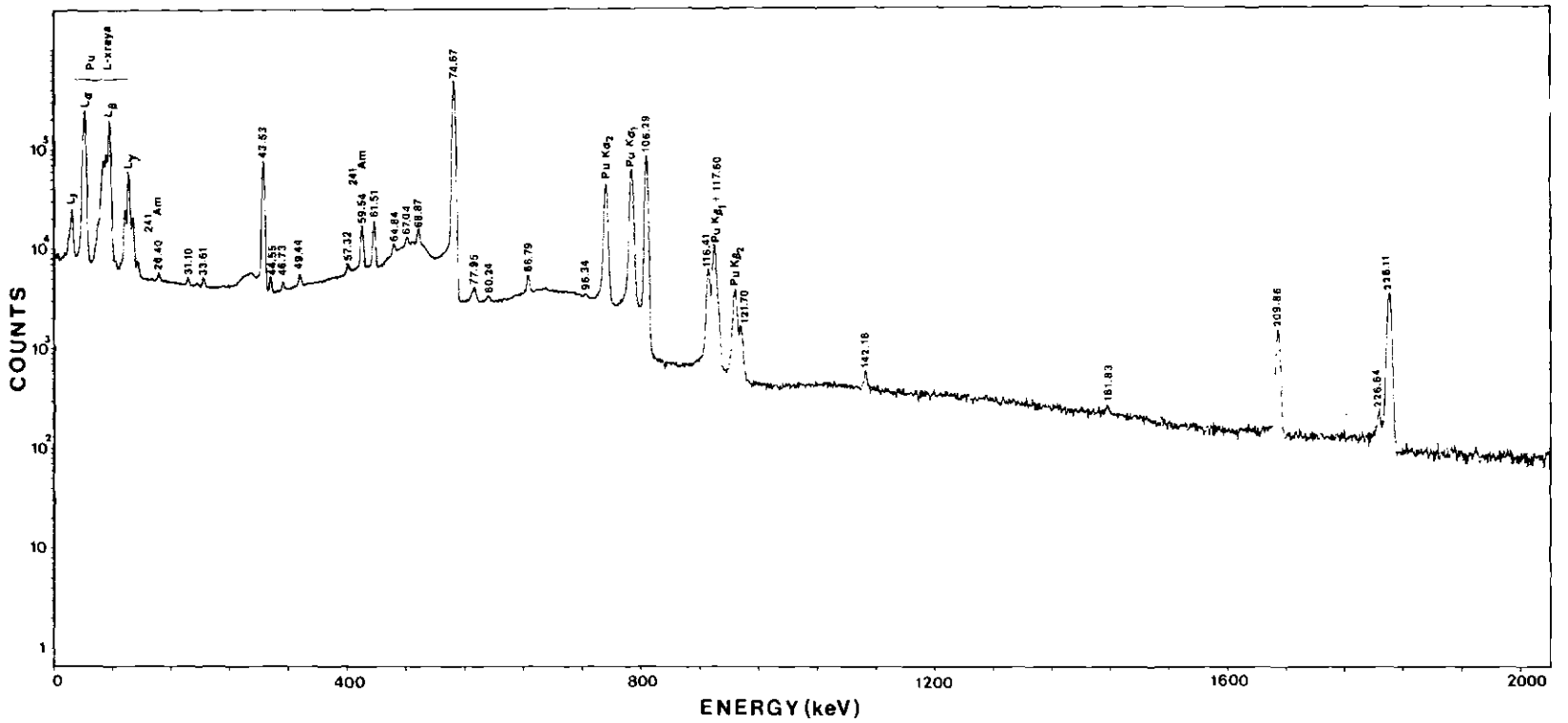

Figure 6. Small Volume Ge(HP) Detector Total Singles Spectrum Using the Electroplated ^{243}Am Source

These gamma transitions were assigned to the ^{239}Pu level scheme for the first time in the present work, based on their observed equilibrium growth rates (see discussion below).

A singles spectrum was also obtained with the large volume (high efficiency) Ge(Li) detector (see Sect. 1.2) over the energy range 40 to 1332 keV using the electroplated ^{243}Am source. This singles gamma-ray spectrum is shown in Fig. 7.

Figure 7 displays the high energy gamma transitions observed in the present work. The Pu K x rays are again prominent in this singles spectrum. Numerous high energy background gammas are present, although a 15 cm lead shield was constructed around the source and detector face to reduce the amount of background radiation. These background gammas have been assigned as indicated.

The ^{239}Np gamma rays at 43.53, 74.67, 86.79, and 142.18 keV are again present in this singles spectrum. The gamma rays at 61.51, 106.29, 209.86, 228.11, 254.46, 272.87, 277.66, 285.54, 216.05, 334.49, 392.3, 497.8, and 504.2 keV are well established transitions in the ^{239}Pu level scheme.

The 385.5 keV gamma ray has been placed in the ^{239}Pu level scheme for the first time in the present work (see Sect. 1.4).

Singles spectra from a freshly prepared ^{243}Am source were taken continuously for 15 hours after chemical separation of the ^{243}Am from its decay products (see Sect. 1.1), and the accumulated results were printed out at 15 minutes, 30 minutes, 1 hour, 5 hours, and 15 hours. Figure 8 displays a composite of these singles spectra which shows the growth of the 2.35 d ^{239}Np daughter decay as it comes into equilibrium with the

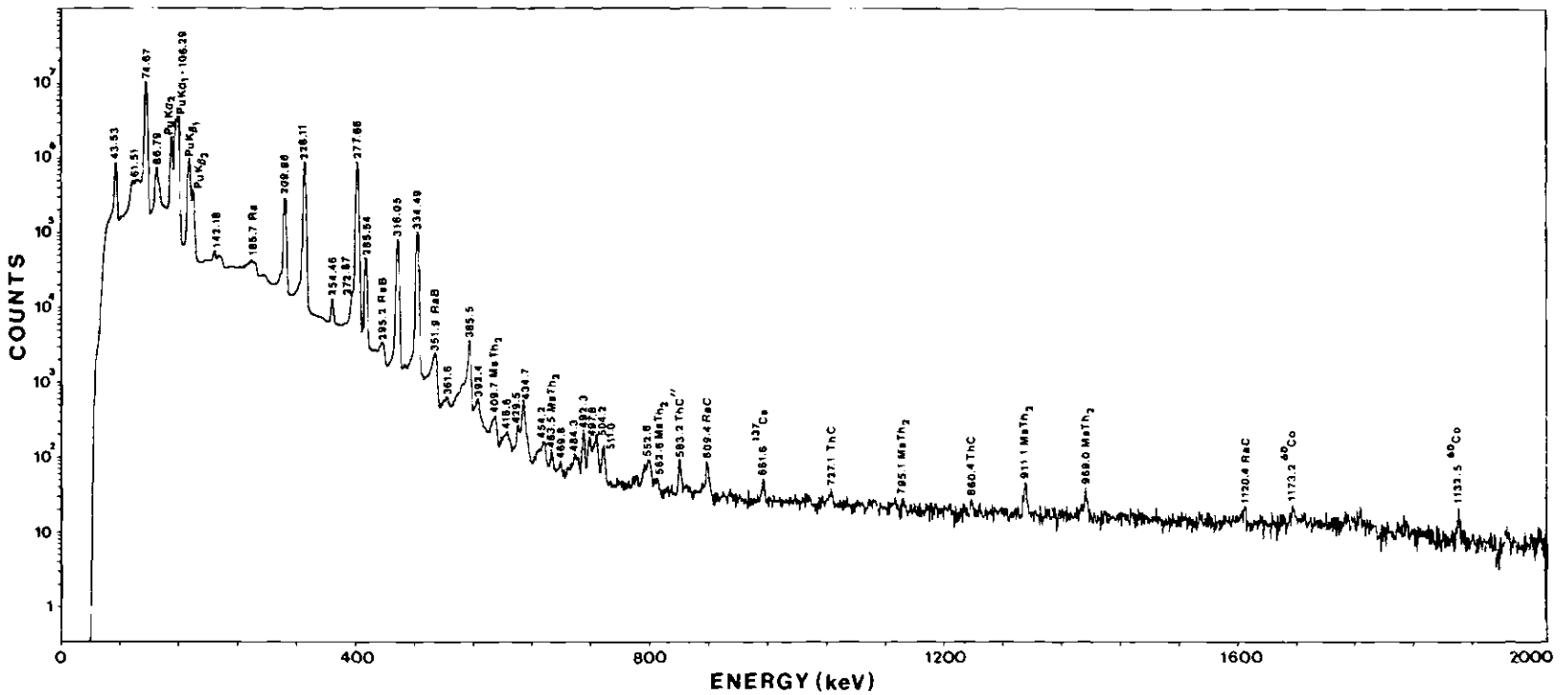

Figure 7. Large Volume Ge(Li) Detector Total Singles Spectrum Using the Electroplated ^{243}Am Source

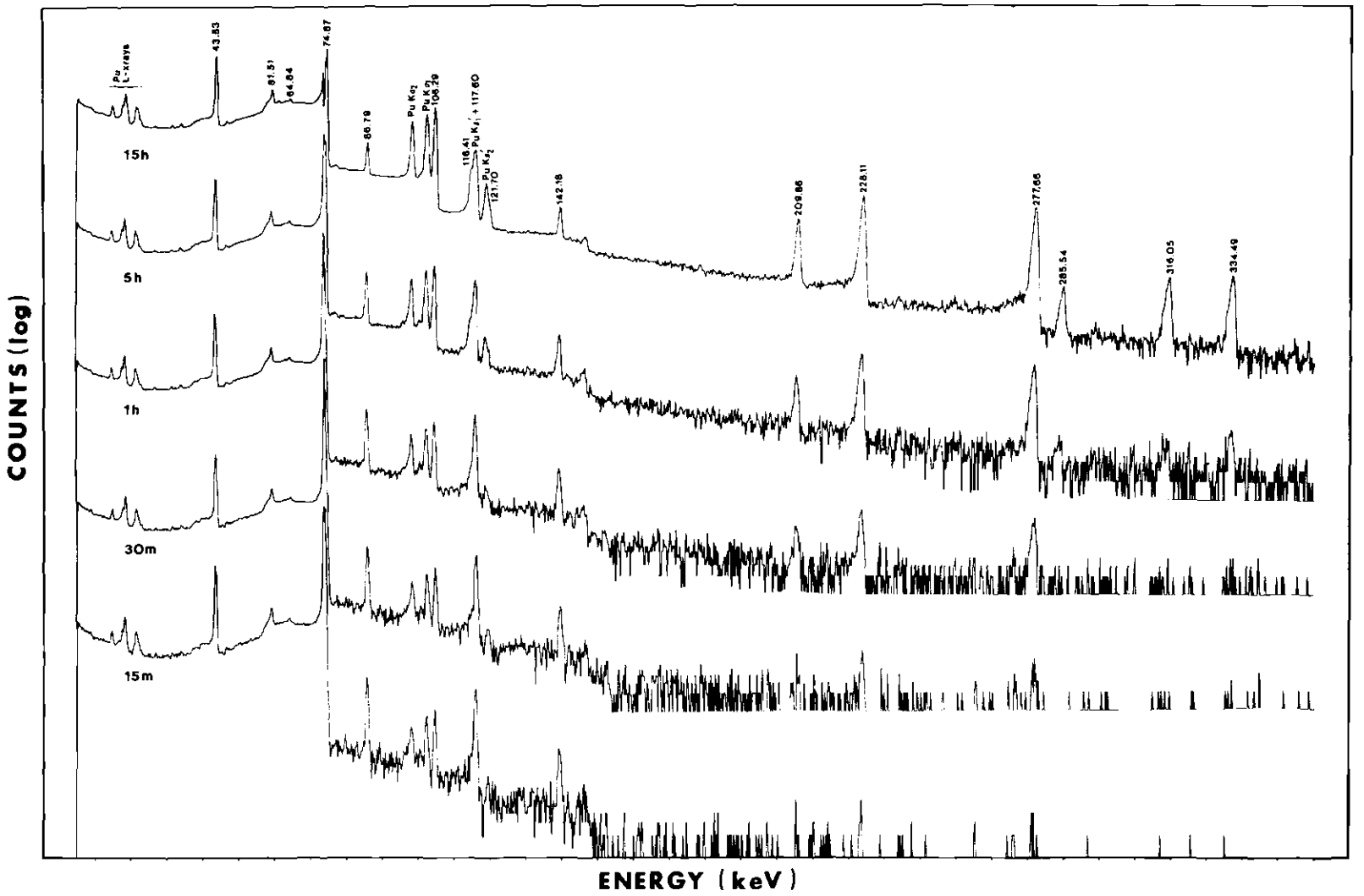

Figure 8. Composite Singles Spectra from Chemically Separated ^{243}Am Source (Taken with the small volume Ge(HP) detector at indicated time intervals after chemical separation.)

7950 year ^{243}Am decay. The relative intensity of the ^{239}Pu K x rays, compared to the intensity of the 43.53 keV ^{239}Np gamma ray (see Fig. 1), was measured as a function of time. This relative intensity growth ratio was used to distinguish gamma rays belonging to ^{243}Am decay from those due to source impurities or to ^{239}Np decay.

From the secular equilibrium growth rate equations, the ratio of photopeak intensities as a function of time is given by:

$$\frac{I_{(\gamma_2)}}{I_{(\gamma_1)}} = \frac{K\lambda_1 \left[t + \frac{1}{\lambda_2}\left(e^{-\lambda_2 t} - 1\right)\right]}{\left(1 - e^{-\lambda_1 t}\right)} \qquad (15)$$

where subscripts 1 and 2 correspond to the parent and daughter, respectively, λ is the decay constant, and K is a constant equal to the ratio of the respective number of gammas per nuclear decay.

The measured ratio, I(Pu Kα's)/I(43.53), as a function of time, followed the growth rate curve predicted by the above equation when the published half-lives for ^{239}Np and ^{243}Am were used.

Comparison of the gamma-ray spectrum from a ^{243}Am source in decay equilibrium (see Figs. 6 and 7) with that obtained from a freshly prepared ^{243}Am source (see Fig. 8) permitted assignment of the gamma rays to decay of ^{239}Np and allowed for exclusion of some of the gamma rays due to source contaminants which were observed in the older electroplated source but not in the freshly separated source. For example, the 68.87 keV and 96.34 keV gamma rays observed in the low energy singles spectrum (Fig. 6) were not present in the spectrum taken from the chemically separated

source (Fig. 8), indicating that these gamma rays are due to contaminants in the electroplated source.

The 117.60 keV ground state transition in ^{239}Np (see Chapter IV, Fig. 13) was masked by the much stronger 117.15 keV Pu $K\beta_1'$ of its daughter. However, from the freshly separated ^{243}Am source, the intensity of the 117.60 keV gamma ray was obtained relative to the 74.67 keV gamma ray from a spectrum taken 15 minutes after chemical separation. The intensity obtained by this method for the 117.60 keV transition is 0.84 ± 0.12 which differs somewhat from the only reported value of 1.2, obtained by α-γ coincidence measurements.[8] No errors were given for this intensity.

Previously unreported gamma rays such as the 116.41 keV transition were identified as belonging to ^{239}Np decay by observing that their growth as a function of time followed that of the K x rays of Pu. However, spectra of some of the weaker gamma rays had such poor statistics that such identification was inconclusive.

1.4 Gamma-Gamma Coincidence Measurements

In principle, the placement of gamma transitions into a decay scheme can be done entirely on the basis of energy and intensity balancing. This has proven to be a valuable technique in many earlier studies of the ^{243}Am decay scheme.[17,18,19] However, many ambiguities may arise by this method, due to existing errors in energy determinations or because of failure to adequately resolve closely spaced photopeak multiplets. Coincidence measurements are useful in that they clearly establish gamma cascade transition relationships in a nuclear decay scheme.

The two-parameter coincidence system depicted in Fig. 9 was used

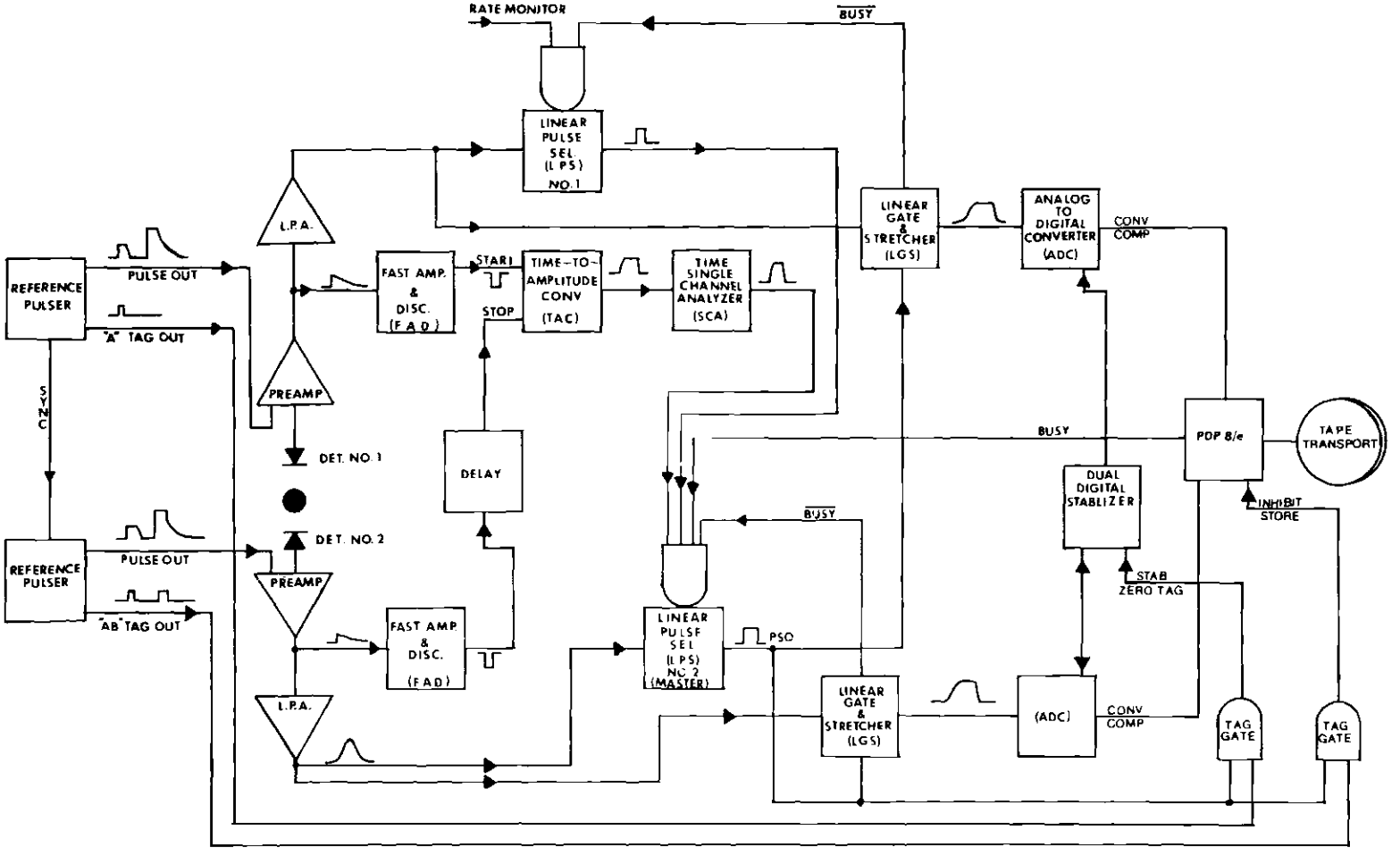

Figure 9. Block Diagram of Gamma-Gamma Coincidence System

to collect coincidence data from ^{243}Am decay using an electroplated source which contained ^{243}Am in equilibrium with its daughters. The coincidence system consisted of two major branches, each composed of a detector, a preamplifier, a linear pulse amplifier (LPA), a linear pulse selector (LPS), a linear gate and stretcher (LGS), and an analog-to-digital converter (ADC). The germanium detectors described in Sect. 1.2 provided their respective preamplifiers with current pulses, directly proportional to the amount of energy given up in the sensitive volume of the germanium crystal by the incident photon. The preamplifier converted this current pulse into a voltage pulse whose amplitude was directly proportional to the deposited energy.

Following the pulse amplifier in each branch of the system was a pulse selector (LPS). This module contained a single-channel analyzer, a pulse-shape discriminator, and a gating circuit which was capable of combining several logic signals to generate an output which controlled the linear gate. Only when the linear gate received an output from the LPS did it allow the pulse to be passed to the ADC. An adjustable delay was included in the pulse selector so that the output signal from one LPS (the master pulse selector) could be used to gate the input to the other LPS. A pulse-shape discriminator was included in each LPS to reduce degradation of system resolution due to pulse pileup (one pulse riding on the tail of a previous pulse).

In this manner, all decisions concerning the acceptability of a particular energy pulse and any coincidence requirements which might have been imposed were made before the pulse was allowed to pass to the ADC.

The linear gate contained a biased amplifier which allowed a fixed

voltage to be subtracted from the amplitude of each pulse. This permitted energies in a particular region of interest to be digitized by the analog-to-digital converter (ADC).

A fast timing system determined whether a prompt coincidence had occurred. The time of occurrence of an event in a detector was determined by a discriminator which generated an output whenever the preamplifier signal exceeded a certain minimum threshold. The output of the small volume Ge(HP) detector (Det. No. 1) was used to start a time-to-amplitude converter (TAC). The output of the large volume, true coaxial Ge(Li) detector (Det. No. 2) was delayed for 110 nanoseconds and used to stop the TAC. The TAC produced an output pulse whose amplitude was proportional to the time interval between these two start and stop signals.

Time resolution was determined by the charge collection time of the detector and preamplifier. The timing window on the single channel analyzer was set to accept a range of TAC output pulse amplitudes corresponding to a coincidence resolving time of about 75 nanoseconds (See Fig. 10). The true-to-chance coincidence ratio was approximately 3 to 1 for these measurements. The TAC output was required to overlap the other

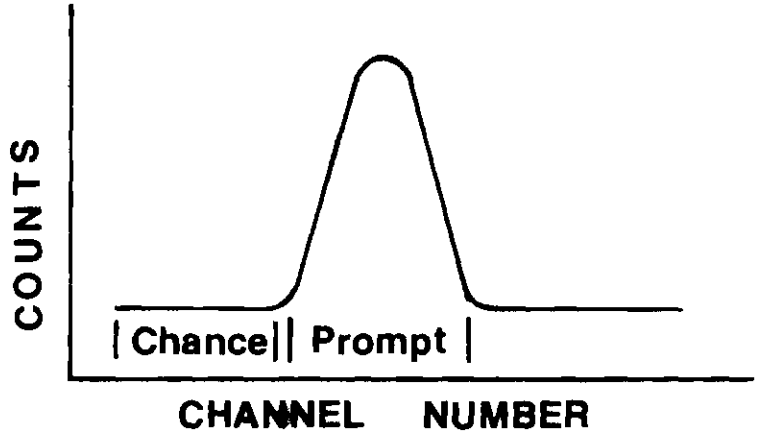

Figure 10. Coincidence Time Spectrum

gating signals at the master pulse selector to permit pulse analysis.

Thus, propagation of a pulse down both branches of the coincidence detection system required simultaneous arrival of signals from the TAC and from the other linear pulse selector at the master pulse selector. Events meeting this fast-slow coincidence condition were then digitized and recorded.

Since coincidence measurements were recorded over a period lasting for several days, a spectrum stabilization system was required to prevent drift of the gain or zero level electronic settings in order to preserve the high resolution of the Ge(Li) detectors. Stabilization was based on the use of two highly stable dual pulsers which introduced reference pulses into each branch of the coincidence system.

A PDP-8/e computer served as the basis of the two-parameter coincidence system. The data buffers were periodically written out onto magnetic tape in event-by-event form. Each event consisted of a twelve-bit integer from each of the two ADC units corresponding to the channel number of the energy of the gamma-ray transition observed in each detector. These event-pairs were stored sequentially as they occurred in a 2048-word memory buffer of the PDP-8/e. When one buffer was filled, it was immediately written onto magnetic tape while data collection continued in a second memory buffer.

These raw event-by-event coincidence data were later sorted into composite spectra which were the total number of events in one detector which had occurred in coincidence with events of any energy in the other detector, i.e., the total spectrum observed in one detector. Gates were then selected corresponding to each photopeak in both composit spectra.

These gates necessarily included the photopeak as well as the underlying Compton background distribution. A correction for this Compton background was obtained by setting windows to the left and/or right of each photopeak. Thus, if the photopeak gate and background gate were of equal width subtraction would yield the true gamma-ray coincidence spectrum. When the photopeak gate and Compton background windows were not of equal width, the correction was adjusted accordingly.

Analysis of the coincidence data was accomplished by computer programs. The raw coincidence data were sorted into composit spectra using program SORT. Another program (SEARCH) was then used to compute the area of each photopeak in the gated spectra.

Two separate coincidence experiments were conducted. The first experiment involved the two detectors described in Sect. 1.2 [the small volume Ge(HP) and the large volume, true coaxial Ge(Li)]. A total of 1,561,000 coincidence events were recorded over a two-day period in this experiment. A second coincidence experiment was then conducted with two large volume, coaxial Ge(Li) detectors* to confirm the high energy gamma coincidence relationships. Approximately 7,077,000 coincidence events were recorded over a four-day period in this experiment. The gamma-gamma coincidence relationships observed in these experiments are presented in Table 3. Those relationships denoted by (C) represent strong coincidences.

As examples of the coincidence data used in compiling Table 3, Figs. 11 and 12 show typical coincidence spectra. Fig. 11 shows the

*The second large volume coaxial Ge(Li) detector has characteristics very similar to those described in Sect. 1.2 for the first large volume detector.

Table 3. Results of Gamma-Gamma Coincidence Experiments*

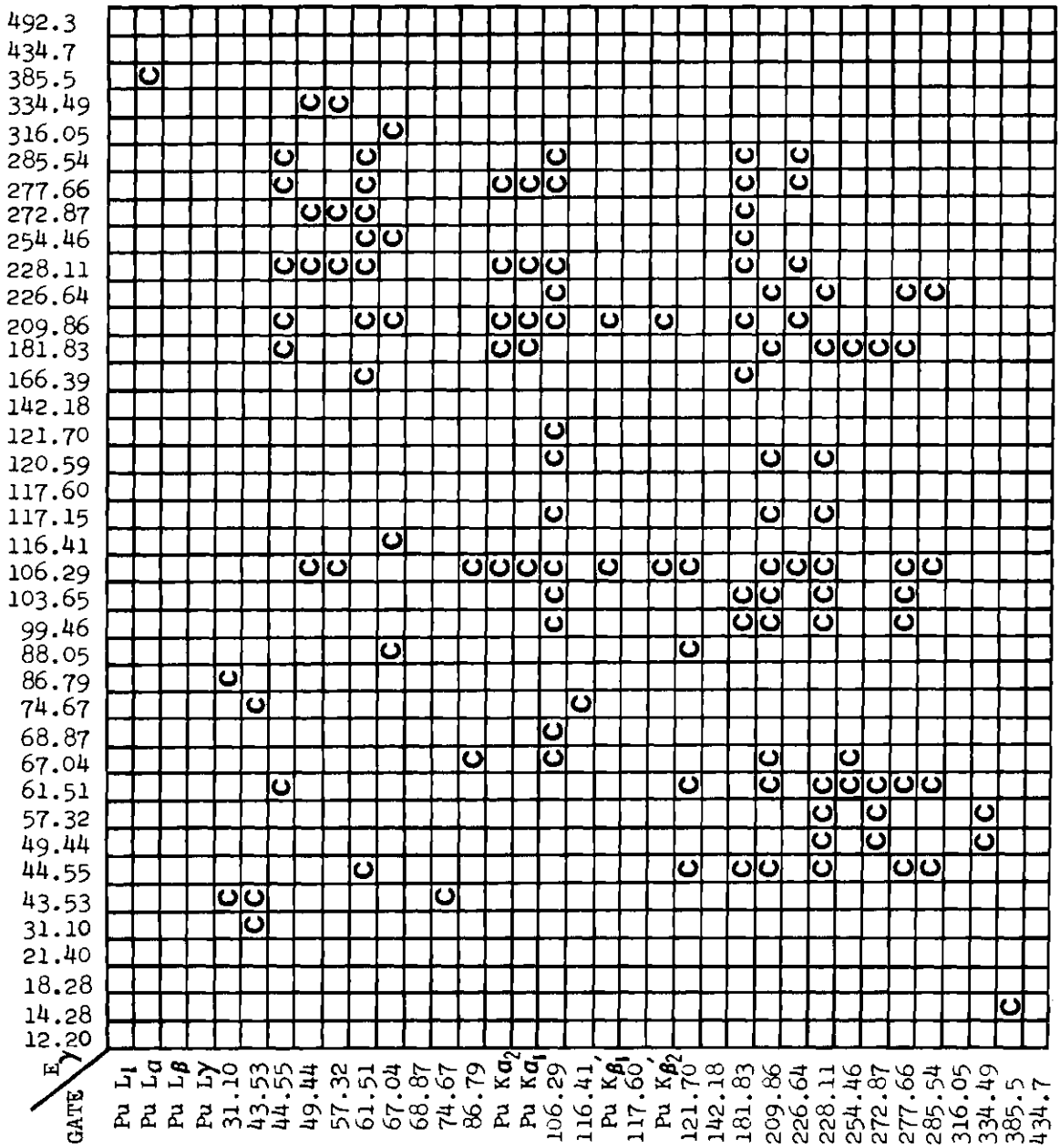

*Energies are in keV. Observed coincidences are indicated by the symbol C.

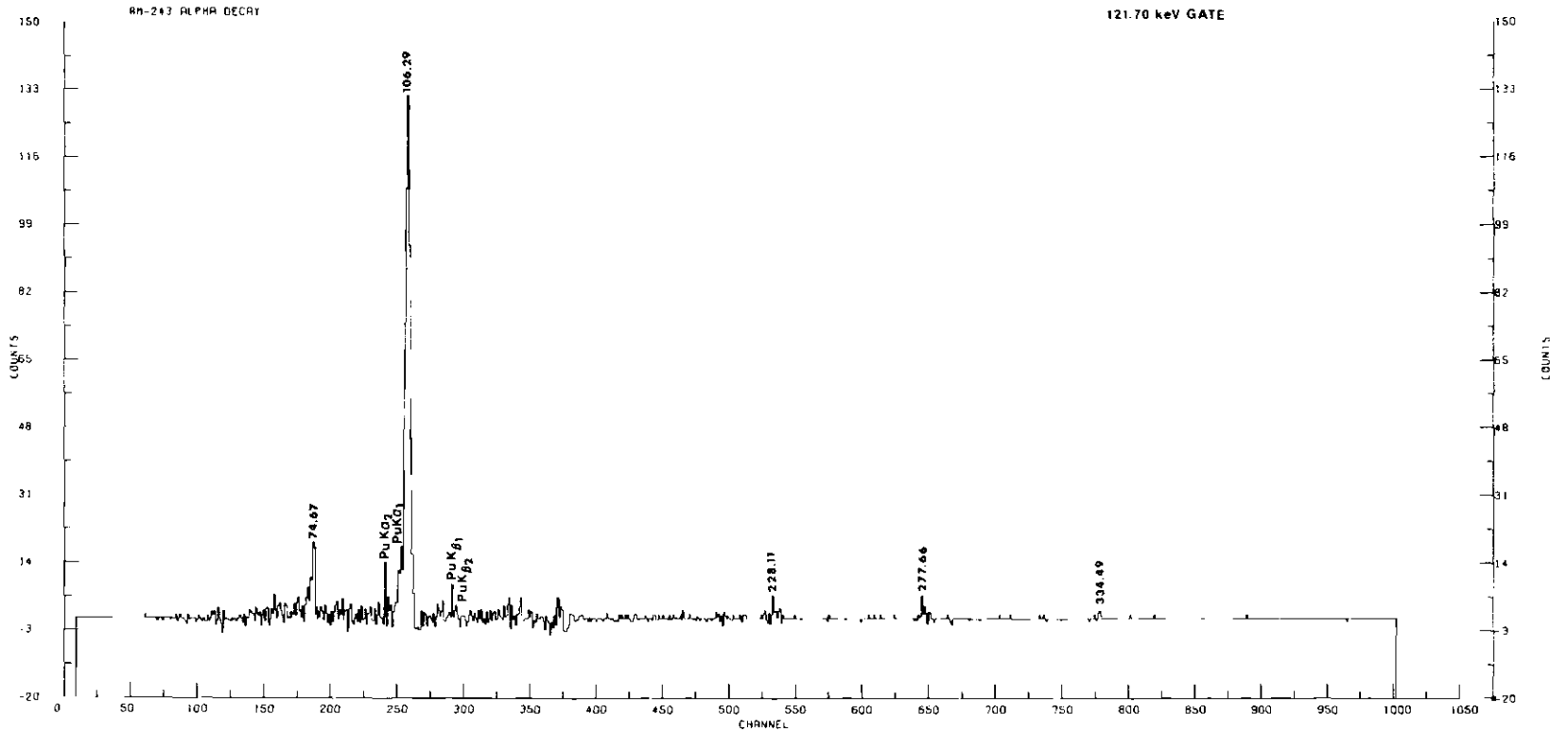

Figure 11. Gamma-Ray Spectrum of 121.70 keV Transition in Coincidence with 106 keV Gamma Rays in ^{239}Pu

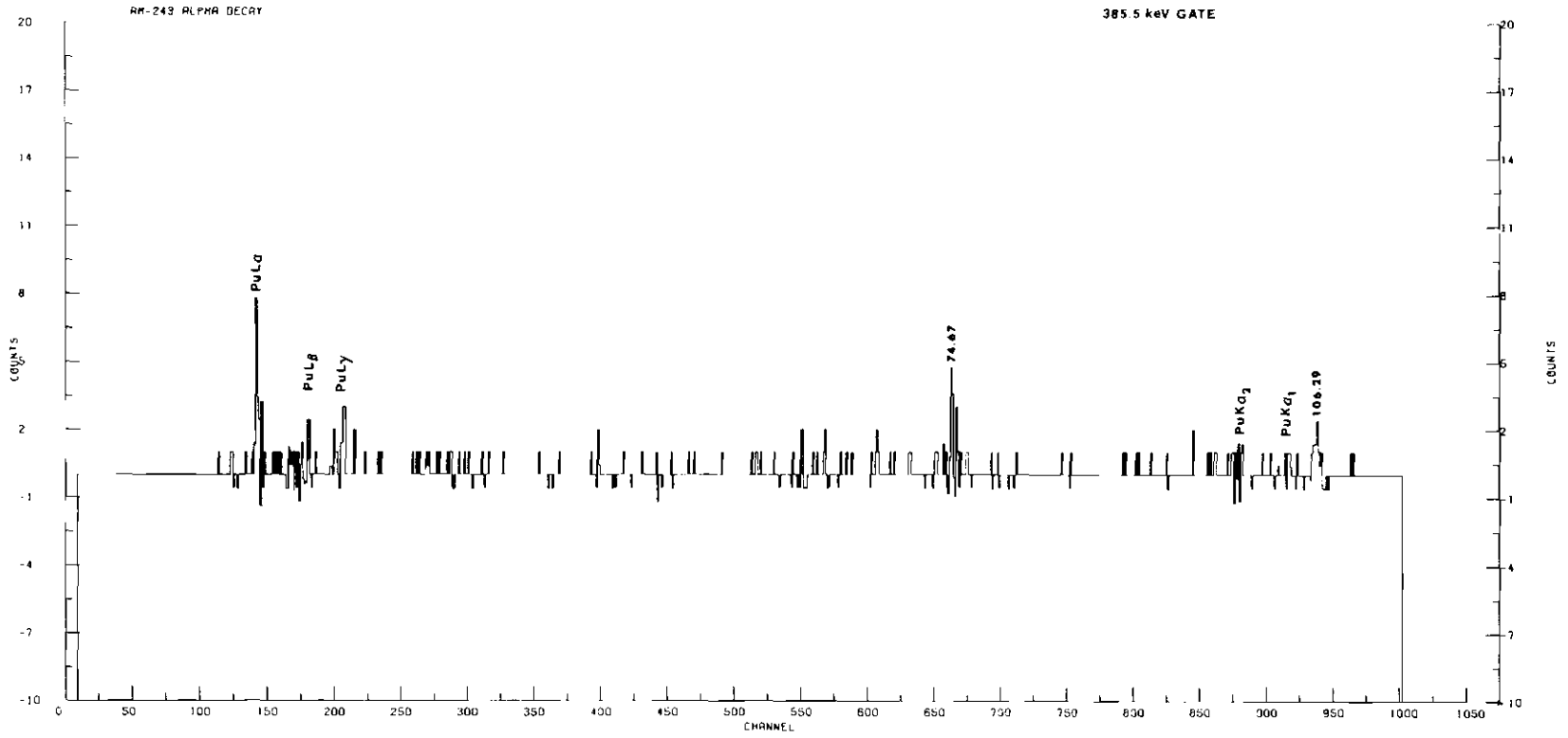

Figure 12. Gamma-Ray Spectrum of 385.5 keV Transition in Coincidence with Lα X Ray in ^{239}Pu

gamma-ray spectrum obtained from the large volume Ge(Li) detector by gating on the previously unplaced 121.70 keV gamma transition in the small volume Ge(HP) detector. This spectrum demonstrates that the 121.70 keV gamma transition occurs in coincidence with the 106.29 keV gamma which is a well known doublet in the ^{239}Pu level scheme (see Chapter IV).

Fig. 12 shows the gated coincidence spectrum of the 385.5 keV gamma ray. This spectrum was obtained from the small volume Ge(HP) detector by gating on the region including the gamma ray in the large volume Ge(Li) detector. The previously unplaced 385.5 keV transition is seen to be in coincidence with the $L\alpha$ x rays of Pu, but not with the $L\beta$ or $L\gamma$ x rays.

$L\alpha$ x rays arise from electron cascade filling of an L_3 subshell vacancy, while $L\beta$ and $L\gamma$ x rays are principally the result of the filling of L_1 of L_2 vacancies. Therefore, coincidence of the 385.5 keV gamma ray with only the Pu $L\alpha$ x ray indicates that it is in coincidence with a gamma ray which is converted totally in the L_3 subshell.

Since there is no photon multipolarity which produces total conversion in the L_3 subshell, a search was made for a possible gamma transition which has enough energy to convert in the L_3 subshell, but is energetically forbidden to convert in the L_1 or L_2 subshells. The only transition between known energy levels in ^{239}Pu which meets these criteria is between the 75.73 and 57.28 keV levels. In fact, the energy difference between the 75.73 and the 461 keV levels corroborates placement of the 385.5 keV gamma transition between these levels.

CHAPTER IV

RESULTS AND DISCUSSION

The present work is the first comprehensive gamma-ray study of the decays of ^{243}Am and ^{239}Np using a two-parameter coincidence spectrometer with high resolution germanium detectors. The combination of an ultra-high resolution small volume detector, Ge(HP), and a high efficiency large volume detector, Ge(Li), allowed many multiplet photopeaks in the spectra to be resolved and measured (See Table 2), and their coincidence relationships to be established for the first time (See Table 3).

The level scheme of ^{239}Pu had been established by study of the beta decay of ^{239}Np,[20,21] electron capture decay of ^{239}Am,[22] and alpha decay of ^{243}Cm.[23,24] However, previous coincidence studies[25,26] confirmed the placement of only four of the many transitions in ^{239}Pu decay.

Because of preferential feeding of the lower excited states of ^{239}Np from ^{243}Am decay, little additional information on this decay was obtained in the present work. However, three of the transitions placed by Engelkemeir[8,9] were confirmed.

From the high resolution singles data, new gamma rays of 116.41, 121.70, and 385.5 keV were observed. These transitions have been assigned to ^{239}Np decay based on radiochemical separation, their observed equilibrium growth rate, and their gamma-gamma coincidence relationships.

The observed 116.41 keV coincidence in the 67.04 keV gated spectrum

confirms placement of this transition between the 193.0 and 75.73 keV levels in the ^{239}Pu decay scheme. Observed coincidences between the 121.70 keV and the 106.29 keV transitions clearly establish that the transition depopulates the 285.44 keV level. Coincidence relationships observed between the Pu Lα x rays and the 385.5 keV transition also confirm the placement of this previously unreported gamma ray.

The proposed level scheme for ^{239}Np is shown in Fig. 13. These levels can be characterized in terms of two intrinsic Nilsson states: the $5/2^+[642]$ ground state and a $5/2^-[523]$ vibrational state at 74.67 keV. Rotational excitations are built upon these intrinsic Nilsson states. The 7/2+ level at 31.142 keV, the (9/2+) level at 71.21 keV, and the (11/2+) level at 123.0 keV represent rotational excitations of the $5/2^+[642]$ ground state. The 7/2- level at 117.66 keV, the 9/2- level at 173.05 keV, the 11/2- level at 241.4 keV, and the (13/2-) level at 320.0 keV represent rotational excitations of the $5/2^-[523]$ state at 74.67 keV.

The present work confirms the existence of the weak 43.1 keV transition between the 7/2- level at 117.66 keV and its band head at 74.67 keV proposed by Engelkemeir.[8] This weak 43.1 keV gamma was found in coincidence with both the 43.53 keV and the 74.67 keV gamma transitions, although it was not resolved from the 43.53 keV photopeak in the high resolution singles spectra.

The remaining very weak gammas shown in Fig. 13 with energies of 50.6, 55.4, 98.5, 169.0, and 195.0 keV were not observed in the present work. They have been seen previously in α-γ coincidence[8] or in conversion electron studies[9] from the decay of ^{243}Am.

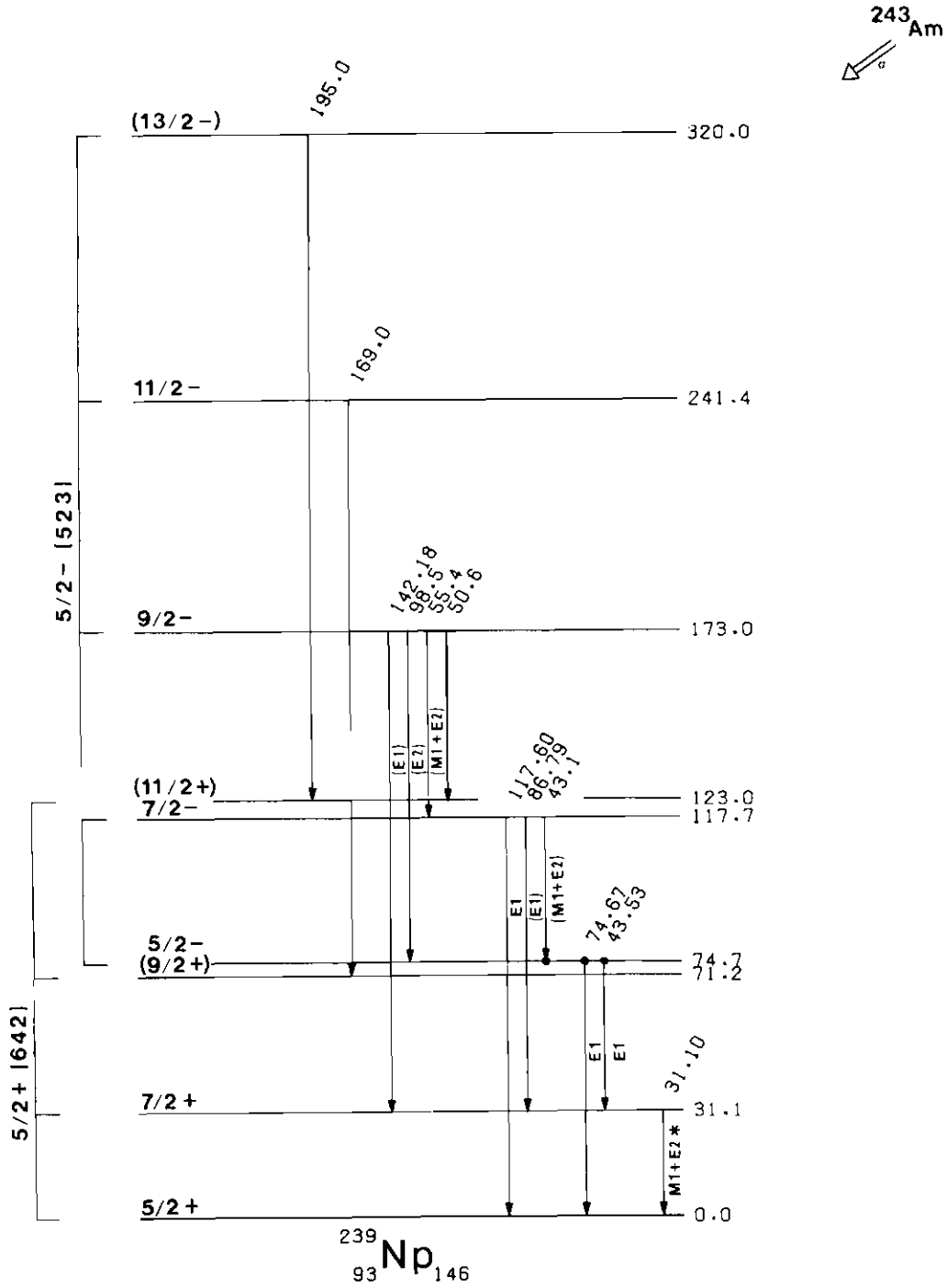

Figure 13. Decay Scheme of ^{239}Np

(Figure shows levels and transitions following α-decay of ^{243}Am studied in the present work. Energies are in keV. Relative photon intensities are given in Table 2. Brackets indicate the two rotational bands based on the $5/2^+[642]$ and the $5/2^-[523]$ Nilsson states as discussed in the text.)

*E2 for the 7/2+ → 5/2+ ground-state transition is less than 30% (see Ref. 27).

The proposed level scheme for ^{239}Pu is shown in Fig. 14. This level scheme has been well established by published work on this nuclide.[20-26] The levels have been characterized in terms of four intrinsic Nilsson states and the rotational excitations of these states.[28] The Nilsson states and their energies are $1/2^+[631]$, ground; $5/2^+[622]$, 285.4 keV; $7/2^-[743]$, 391.5 keV; and $1/2^-[501]$, 469.8 keV.

The 3/2+ level at 7.85 keV, the 5/2+ level at 57.28 keV, the 7/2+ level at 75.73 keV, the 9/2+ level at 163.79 keV, and the proposed (11/2+) level at 193.0 keV[28] are rotational excitations based upon the ground state Nilsson band of $1/2^+[631]$. Other rotational levels have been assigned to Nilsson states as indicated in Fig. 14.

The present work confirms 24 of the gamma-gamma coincidence relationships in the ^{239}Pu level scheme for the first time and places new gamma transitions with energies of 116.41, 121.70, and 385.5 keV.

The placement of the 121.70 and 116.41 keV transitions confirms for the first time that the 193.0 keV level has a spin-parity of 11/2+. The decay characteristics of the 285.4 keV 5/2+ level, which is now known to decay to states with spins of 1/2, 3/2, 5/2, 7/2, and 9/2, but not to the level at 193.0 keV, indicate that the spin of the 193.0 keV level must be larger than 9/2. Additional evidence is obtained by the observed presence of the 116.41 keV transition to the 7/2+ level at 75.73 keV, but not to the 5/2+ level at 57.28 keV or to lower spin states, indicating that the spin is 11/2+.

Placement of the 385.5 keV transition confirms for the first time that the 11/2+ level at 461.0 keV is fed in this decay. This level was known to be fed weakly (0.02%) by the alpha decay of ^{243}Cm,[23,24] but had

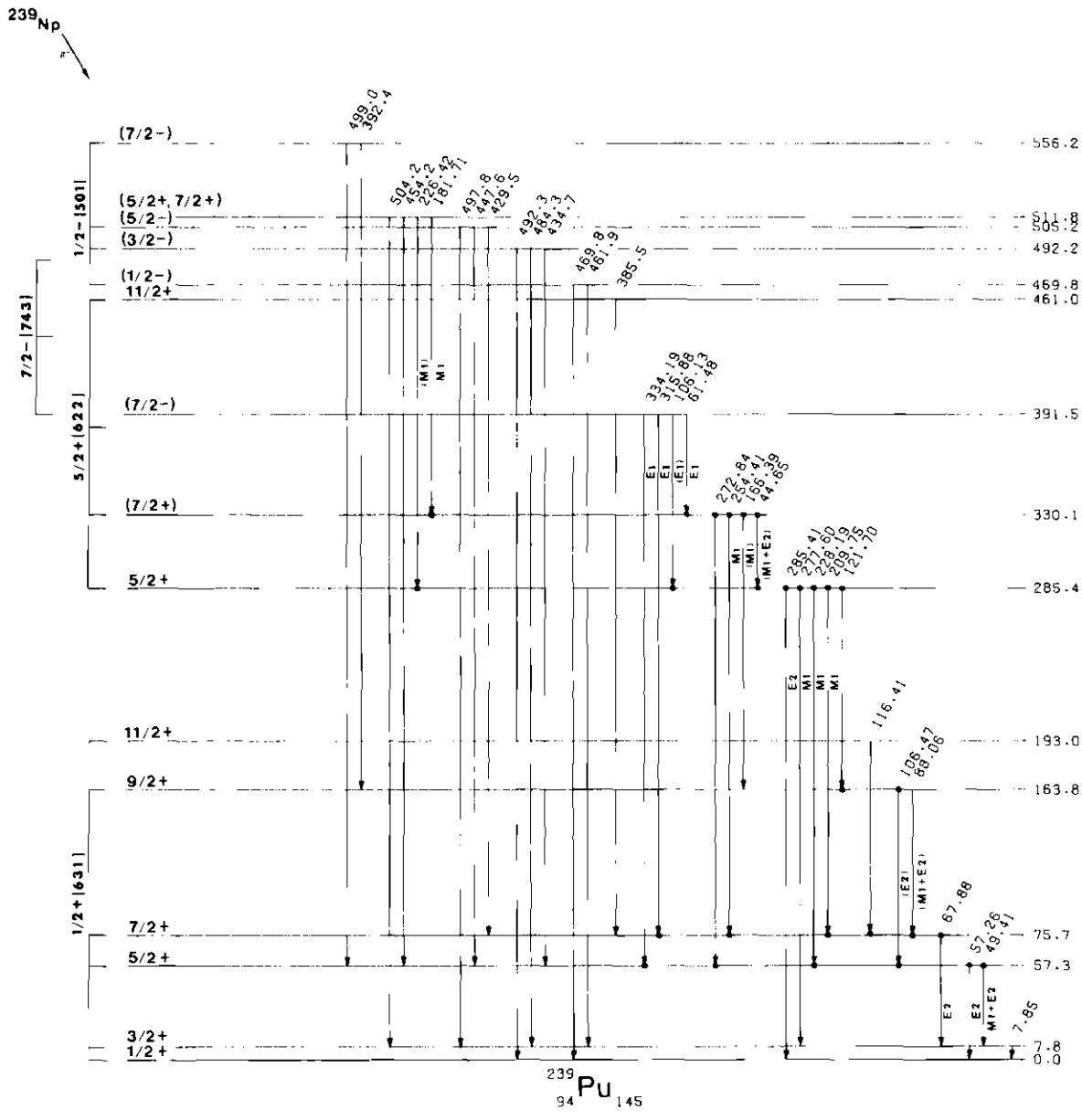

Figure 14. Decay Scheme of ^{239}Pu

(Figure shows levels and transitions following β^- decay of ^{239}Np studied in the present work. Energies are in keV. Relative photon intensities are given in Table 2. Brackets indicate the four rotational bands based on the $1/2^+$ [631], the $5/2^+$ [622], the $7/2^-$ [743], and the $1/2^-$ [501] Nilsson states as discussed in the text.)

not previously been observed from the beta decay of ^{239}Np.

Weak 361.6, 418.6, and 552.8 keV gammas were observed in the singles measurements taken with the large volume Ge(Li) detector (see Fig. 7), but could not be placed in the decay scheme based on energy fitting. They were not observed in the coincidence measurements.

In conclusion, this work has verified most of the previously reported transitions in the level schemes of ^{239}Np and ^{239}Pu. The placement of three new transitions enables us to definitely assign a spin to the 193.0 keV level of 11/2 and to firmly establish the 461.0 keV level in ^{239}Pu. The weak 43.1 keV gamma transition from the 117.66 keV level in ^{239}Np has been confirmed.

The results of the present work provide confirmation of previous experimental gamma-ray measurements for these decay schemes. Data such as these gathered by singles and gamma-gamma coincidence spectroscopy are useful in positively establishing nuclear level schemes.

As more experimental data are compiled, trends such as consistent energy level spacings, transition probabilities, and decay modes may be detected. These trends may suggest more about the physical nature of the nucleus and may provide insight for the construction of working theoretical nuclear models.

BIBLIOGRAPHY

1. G. T. Seaborg, R. A. James, and L. O. Morgan, The Transuranium Elements, McGraw-Hill, Inc., New York, 1949.

2. A. Ghiorso, R. A. James, L. O. Morgan, and G. T. Seaborg, Phys. Rev. 78, 472 (1950).

3. E. K. Hyde, I. Perlman, and G. T. Seaborg, The Nuclear Properties of the Heavy Elements, Vol. II, Prentice-Hall, Inc., Englewood Cliffs, N. J., 1964.

4. Nuclear Data Sheets, National Research Council-National Academy of Science, 5-5-26 (January, 1972).

5. M. G. Mayer, Phys. Rev. 75, 1969 (1949).

6. O. Haxel, J. H. D. Jensen, and H. E. Suess, Phys. Rev. 75, 1766 (1949).

7. S. G. Nilsson, K. Danske Vidensk. Selsk. Mat.—Fys. Medd. 29, #16 (1955).

8. J. R. Van Hise and D. Engelkemeir, Phys. Rev. 171, 1325 (1968).

9. D. Engelkemeir, Phys. Rev. 181, 1675 (1969).

10. S. G. Nilsson, Lecture Notes: Nuclear Structure, Fission, and Superheavy Elements, UCRL-18355 (1968) (unpublished).

11. F. S. Stephens, F. Asaro, and I. Perlman, Phys. Rev. 113, 212 (1959).

12. A. M. Poskanzer and B. M. Foreman, J. Inorg. Nucl. Chem. 16, 323 (1961).

13. G. A. Burney and R. M. Harbour, The Radiochemistry of Neptunium (to be published).

14. I. Ahmad and W. Wahlgren, Nucl. Instr. and Meth. 99, 333 (1973).

15. J. S. Hansen, J. C. McGeorge, D. Nix, W. D. Schmidt-Ott, I. Unus, and R. W. Fink, Nucl. Instr. and Meth. 106, 365 (1973).

16. K. J. Blinowska, P. G. Hansen, H. L. Nielsen, O. Schult, and K. Wien, Nucl. Phys. 55, 331 (1964).

BIBLIOGRAPHY (Continued)

17. F. Asaro, F. S. Stephens, J. M. Hollander, and I. Perlman, Phys. Rev. 117, 492 (1960).

18. S. A. Baranov, V. M. Kulakov, and V. M. Shatinsky, Nucl. Phys. 56, 252 (1964).

19. C. M. Lederer, J. K. Poggenburg, F. Asaro, J. O. Rasmussen, and I. Perlman, Nucl. Phys. 84, 481 (1966).

20. J. M. Hollander, W. G. Smith, and J. W. Mihelich, Phys. Rev. 102, 740 (1956).

21. G. T. Ewan, J. S. Geiger, R. L. Graham, and D. R. MacKenzie, Phys. Rev. 116, 950 (1959).

22. W. G. Smith, W. M. Gibson, and J. M. Hollander, Phys. Rev. 105, 1514 (1957).

23. F. Asaro, S. G. Thompson, and I. Perlman, Phys. Rev. 92, 694 (1953).

24. F. Asaro, S. G. Thompson, F. S. Stephens, Jr., and I. Perlman, Bull. Am. Phys. Soc. 2, 393 (1957).

25. R. L. Graham and R. E. Bell, Phys. Rev. 83, 222 (1951).

26. D. Strominger and J. O. Rasmussen, Phys. Rev. 100, 844 (1955).

27. W. D. Schmidt-Ott, J. C. McGeorge, and R. W. Fink, Z. Physik 255, 161 (1972).

28. D. W. Davies and J. M. Hollander, Nucl. Phys. 68, 161 (1965).